

Anticancer Activity of Doxorubicin Loaded PBMA-b-POEGMA Micelles Against MCF7 Breast Cancer Cells and HepG2 Liver Cancer Cells

Hamideh Gharnas-Ghamesh¹, Mojtaba Masoumi^{1*}, Vahid Erfani-Moghadam^{2,3}

1. Department of chemical engineering, Ayatollah Amoli Branch, Islamic Azad University, Amol, Iran
2. Medical Cellular and Molecular Research Center, Golestan University of Medical Sciences, Gorgan, Iran
3. Department of Medical Biotechnology, School of Advanced Technologies in Medicine, Golestan University of Medical Sciences, Gorgan, Iran

Article Type:

Original Article

Article History:

Received: 27 Jul 2021

Revised: 25 Aug 2021

Accepted: 4 Sep 2021

*Correspondence:

Mojtaba Masoumi,

Department of chemical
engineering, Ayatollah Amoli
Branch, Islamic Azad University,
Amol, Iran

m.masoumi@iauamol.ac.ir



DOI: [10.29252/jorjanibiomedj.9.3.49](https://doi.org/10.29252/jorjanibiomedj.9.3.49)

Abstract

Background and Objective: Cancer is one of the most serious diseases. Doxorubicin is a type of chemotherapy drug used to treat a variety of cancers. However, its side effects have limited its use. The aim of this study was to synthesize and evaluate polymer micelles containing doxorubicin and evaluate its toxicity on MCF7 breast cancer cells and HepG2 liver cancer cells.

Material and Methods: For this purpose, PBMA-b-POEGMA diblock copolymer was first synthesized using the RAFT method and confirmed by GPC. Dynamic light scattering (DLS) and Transmission electron microscope (TEM) were used to observe the morphology, size, and polydispersity of the micelles. In addition, in vitro cytotoxicity of DOX-loaded polymeric micelles against MCF7 cells and HepG2 cells were assessed. Furthermore, cell uptake and apoptosis assay of DOX-loaded polymeric micelles against MCF7 cells were evaluated.

Results: The TEM image revealed that the nanoparticles were spherical and uniform. The particle size and polydispersity measured by DLS were 35 nm and 0.13, respectively. The drug encapsulation efficiency and drug loading contents were $50 \pm 3.46\%$ and $4.53 \pm 0.29\%$, respectively. The drug release rate was reported 69% in saline phosphate buffer (pH 7.4) within 24 hours. The results showed that micelles containing doxorubicin had a greater effect on MCF7 cell viability than the free drug. The MTT assay demonstrated that micelles were biocompatible to HepG2 cells while DOX-loaded micelles showed significant cytotoxicity. The IC₅₀ of doxorubicin-loaded micelles against MCF7 cells were obtained to be 0.5 µg/ml. It was further shown that micelles containing doxorubicin had higher cell uptake and apoptosis than free drugs on MCF7 cells.

Conclusion: These polymeric micelles are an ideal candidate to deliver anticancer agents into breast cancer cells.

Keywords: Micelles [MeSH], Doxorubicin [MeSH], Polymerization [MeSH], Drug Carriers [MeSH], MCF7 Cells [MeSH]

Highlights

Doxorubicin is a type of drug used to treat cancers. Polymeric micelles are an ideal candidate to deliver anticancer agents into cancer cells.

Introduction

Nanotechnology has emerged as a promising approach for targeted drug delivery and cancer therapy (1). Numerous attempts have been made to study anticancer efficacy of different nanocarriers platforms such as polymeric micelles (2), liposomes (3), nanovesicles (4), and nanogels (5). Polymeric micelles are self-assembled nanostructures comprised from amphiphilic block copolymers which possess core-corona structure with a narrowly distributed nano-size (10-100 nm). Polymeric micelles are attractive for drug delivery applications due to their nano-sizes and the high loading capacity of hydrophobic drugs (6). These vesicular structures are attractive vehicles for increasing bioavailability of hydrophobic drugs in drug delivery applications (7, 8). Drug delivery systems using polymeric micelles as drug carriers can escape from the reticuloendothelial system (RES) due to their unique properties and accumulate in tumor tissue through the enhanced permeability and retention (EPR) effect (9). Several anti-cancer formulations under clinical trials prove the potency of micellar structures in delivering drugs (10, 11). Doxorubicin is one of the most commonly used hydrophobic cancer drugs in the treatment of various cancers (12-14), but due to the lack of specific targeting for tumor cells DOX usually induced side effects, which restricted the clinical applications (14). In order to overcome that limitation and reduce its toxicity, different nanocarriers such as polymeric nanomaterials for DOX delivery have been developed (15, 16).

Controlled radical polymerization (CRP) is an appropriate approach to the synthesis of well-defined block copolymers with precise molecular weights and low polydispersity (17, 18). Among different CRP techniques, reversible addition-fragmentation chain-transfer polymerizations

(RAFT) is one of the most reliable processes to controlled delivery and activity in the physiological environment due to the polymerization of a broad range of monomers with no special limitations in the reaction conditions (19-21).

In this work, PBMA-b-POEGMA block copolymers were synthesized for DOX delivery via RAFT polymerization. Then self-assembly behavior of block copolymers, loading of DOX in the micelle, and release of DOX on the micelle were investigated. In addition, in vitro cytotoxicity of DOX-loaded polymeric micelles against MCF7 cells and HepG2 cells were assessed. Furthermore, cell uptake and apoptosis assay of DOX-loaded polymeric micelles against MCF7 cells were evaluated.

Materials and Methods

• Materials

Oligo ethylene glycol methyl ether methacrylate(OEGMA) (Mw=475 g/mol), n-butyl methacrylate (BMA) were purchased from Sigma. Hexane, 1,4-dioxane, dichloromethane (DCM), diethylether, methanol, N,N-dimethylformamide (DMF), N,N-dimethylacetamide (DMAc), 2,2'-Azobis(2-methylpropionitrile) (AIBN), 4-Cyano-4-(phenylcarbonothioylthio)pentanoic acid, toluene, acetonitrile, doxorubicin hydrochloride, hexylamine (HEA), and triethylamine (TEA) were purchased from Sigma. Dialysis membrane (MWCO: 10000 Da) was purchased from Spectrum® Laboratories.

For biological assays, cell culture medium (RPMI-1640), trypsin, FBS, Dulbecco's PBS, and penicillin-streptomycin were purchased from Thermo Fisher Scientific (Waltham, MA, USA). Annexin V Apoptosis Detection kit was purchased from BioLegend (Shanghai, China). MCF7 (human breast adenocarcinoma cell line) and HepG2 cells (human liver cancer cell line) were obtained from Pasteur Institute (Tehran, Iran). 3-(4,5-dimethylthiazol-2-yl)-2,5-diphenyltetrazolium bromide (MTT) was purchased from Sigma (USA).

- **Synthesis of PBMA homopolymer**

Hydrophobic PBMA homopolymers were prepared using 4-cyanopentanoic acid dithiobenzoate (CPADB) as a chain transfer agent (CTA) and 2,2'-azobisisobutyronitrile (AIBN) as initiator. BMA (4 mol/L), CPADB (8 mmol/L), and AIBN (2 mmol/L) were dissolved in 3 mL toluene. The flask was subsequently degassed by purging nitrogen through the solution. The reaction was allowed to proceed at 65 °C for 8 h. After the polymerization, polymers were precipitated in an excess of methanol/water mixture and dried under vacuum.

- **Synthesis of PBMA-b-POEGMA block copolymer**

PBMA-b-POEGMA diblock copolymers were synthesized using PBMA as macro-CTA. PBMA (20 mmol/L), AIBN (3 mmol/L), and POEGMA (0.2 mol/L) were dissolved in 8 mL 1,4-dioxane and the solution was degassed. The polymerization was conducted at 65 °C for 4h. After polymerization, the solution was precipitated in excess hexane and then dried under vacuum. The synthesis procedures of block copolymer were exhibited in Scheme 1.

- **Characterization of block copolymer**

Synthesized polymers were analyzed by gel permeation chromatography (GPC). Gel permeation chromatography (GPC) was used to determine the molecular weight and molecular weight distribution of homo and block copolymers. A Shimadzu modular system comprising a SIL-10AD auto injector, PSS Gram 30 Å and 100 Å (10 µM, 8x300 mm) columns was used.

- **Preparation and characterization of polymeric micelles**

Dox-loaded micelle was prepared by dialysis as described in previous studies (22). The DOX.HCl (3mg, 1eq) was dissolved in 1 ml DMAc and mixed with triethylamine (TEA, 5eq) stirred overnight at 37 °C in the dark to remove the hydrochloride. Then 30 mg/mL of block copolymers in 1,4-dioxane were added into DOX

solution (3 mg in DMAc) and stirred at room temperature for 2 h. The mixture solution was dialyzed against water (MWCO: 10000) at room temperature for 72 h. The distilled water was replaced every 3 h. After dialysis, the solution was collected and dried by a freeze dryer system to obtain micelles. Blank micelles are prepared in a similar method without the presence of drug. The hydrodynamic diameter (Dh) and polydispersity indexes (PDI) were determined at 25°C by a dynamic light scattering (DLS) instrument with ZetaSizer (Nano-ZS) (Malvern Instruments, Worcestershire, UK) using an argon laser beam at 633 nm and a 90° scattering angle. Transmission electron microscope (TEM) (EM10C; Carl Zeiss Meditec AG, Jena, Germany) was used to observe the morphology, size, and polydispersity of the micelles. A small drop of the sample solution was deposited on to a copper grid covered by 0.2% polyvinyl formal (Vinylec K). The grid was allowed to dry at room temperature. UV-visible spectrophotometry was used to investigate DOX concentration. UV-visible light absorbance of the solutions was measured by a Thermo Scientific Evolution 201 UV-visible spectrophotometer in the range between 200 nm and 600 nm using quartz cuvettes.

- **Physical encapsulation of DOX in micelles**

To determine the drug loading content (DLC) and drug loading efficiency (DLE), the dried DOX-loaded micelle dissolved in DMAc:1,4-dioxane mixture (1:1 v/v) and analyzed with UV/Vis spectrometry at an absorbance at 485 nm. A DOX calibration curve was prepared by different determined DOX concentrations in DMAc: 1,4-dioxane solutions. DLC and DLE were calculated according to the following formulae:

$$\text{DLC (wt\%)} = (\text{weight of loaded drug} / \text{total weight of the polymer and loaded drug}) \times 100$$

$$\text{DLE (wt\%)} = (\text{weight of loaded drug} / \text{weight of the drug in feed}) \times 100$$

- **In vitro release study of DOX from micelles**

A total of 3 mL of DOX-loaded polymeric micelles was transferred to a dialysis bag (MWCO = 10000 Da). It was immersed in 40 mL of

phosphate buffer (pH 7.4) in a shaking water bath at 37 °C. 2 mL of the solution was withdrawn and replaced with an equal volume of fresh medium at predetermined time intervals. The amount of DOX released from micelles was determined with UV measurements.

• *MTT assay*

The cytotoxicity of DOX-loaded micelles and free DOX was determined by the MTT assay. Briefly, MCF7 and HepG2 cells were seeded at a density of 10×10^3 cells/well in 96-well plates and cultured in RPMI supplemented with 10% fetal bovine serum (FBS, Thermo Scientific) and 1% penicillin–streptomycin at 37°C for 24 h. After removing the medium, the cells were incubated with the different concentrations of free DOX and DOX-loaded micelles. After 24 h at 37°C, 10 μ L of MTT solution (5 mg/mL) was added to each well. After four hours incubation, the solutions were removed, and 100 μ L of DMSO was added to each well. The absorbance was measured at 490 nm by an ELISA reader (Awareness Technology Chromate® Microplate Reader). Relative cell viability was calculated by the dividing the absorbance of the treated cells to the absorbance of non-treated cells $\times 100\%$.

• *Cellular uptake of micelles*

Cellular uptakes of the DOX-loaded micelles were analyzed by flow cytometry (FACS Calibur, BD Biosciences, USA). For flow cytometry analysis, MCF7 cells were seeded at a density of 2×10^5 cells/well in 24-well plates and cultured for 24 h. Then free-DOX and DOX-loaded micelles were added and incubated for 4 h at a DOX concentration of 5 μ g/mL. The cells were washed three times with PBS and suspended in 0.5 mL of PBS containing 0.1% sodium azide. The cells were analyzed using flow cytometry at the FL2-channel (excitation 488 nm and emission 575 nm). For each sample, 10,000 events were collected and cells cultured under normal conditions were used as control.

• *Apoptosis analysis*

The apoptotic index of each sample was measured through flow cytometry assays using FITC

Annexin V and PI staining kits (BioLegend®, San Diego, CA, USA) according to the manufacturer's instructions. Briefly, MCF7 cells were seeded (0.2×10^6 cells/well) into 24-well plates and allowed to adhere overnight before treatments. MCF7 cells were incubated with free-DOX and DOX-loaded micelles at a DOX concentration of 5 μ g/mL. After 24 hours, cells were washed twice with cold BioLegend's cell staining buffer and then resuspended in Annexin V binding buffer. Three microliters of Annexin V and six microliters of PI solution were added. After incubating of cells in the dark, 400 microliters of Annexin V binding buffer was added to each tube and analyzed by flow cytometer (BD Biosciences, San Jose, CA, USA). The data were evaluated using a BD Accuri™ C6 software (BD Biosciences).

• *Statistical analysis*

Results were presented as mean \pm the standard deviation (SD) or mean \pm the standard error (SE) of mean. Statistical significance among groups was determined by Student's t-test. A P-value below 0.05 was considered statistically significant.

Results

• *Characterization of the polymers*

For each sample, the number-average molecular weight (M_n) and PDI were determined by GPC (Fig 1). The PDI values of the homopolymer and block copolymer are PDI=1.2 and PDI=1.28, respectively. As shown in Table 1, the molecular weights of PBMA-b-POEGMA diblock copolymers showed a relatively low polydispersity.

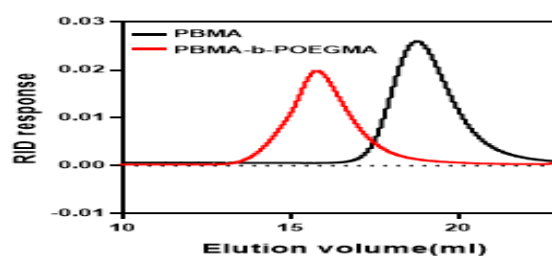


Figure 1. GPC graphic of homo (PBMA) and diblock copolymer (PBMA-b-POEGMA).

• Characterization of polymeric micelles

The dialysis was used to form micelles from the synthesized amphiphilic diblock copolymers. The morphology, size, and particle distribution of the blank micelles and DOX-loaded micelles determined by TEM and DLS (Fig 2, 3). The TEM image revealed that the blank nanoparticles were spherical and uniform and a mean diameter of 20 nm (Fig 2). Furthermore, the DLS results of blank micelles showed a narrow size distribution around 35 nm and PDI of 0.13 (Fig 3). The particle size resulted from DLS is slightly larger than the value achieved from TEM analysis, due to the particle accumulation in aqueous medium (23). As shown in Fig. 3b, after loading of DOX, micelles have larger sizes. The DLS result shows that the size of the DOX-loaded polymeric micelles is 45 nm and the size distribution is 0.18.

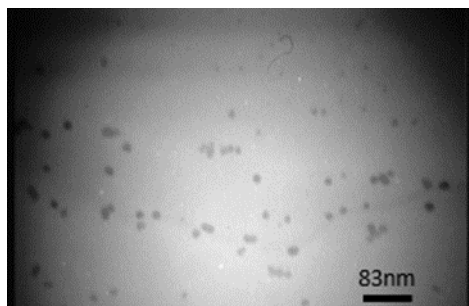


Figure 2. TEM image of PBMA-b-POEGMA blank micelles.

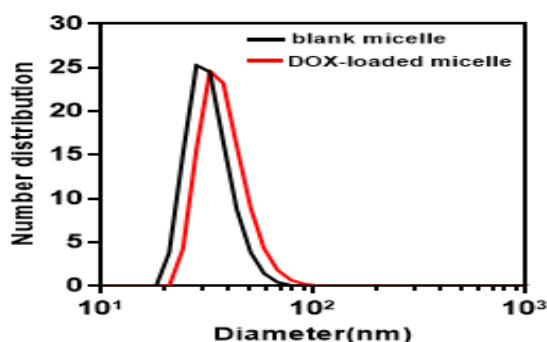


Figure 3. The size distribution of a) blank micelles, and b) DOX-loaded micelles determined by DLS

• Physical encapsulation of DOX in micelles

The DLE and DLC of the DOX-loaded polymeric micelles are 4.53 ± 0.29 % and 50 ± 3.46 %, respectively, when the feed ratio of polymer to DOX is 10: 1.

• In vitro release study of DOX from micelles

As shown in Fig 4, the release of drug from the micellar nanocarriers into the media occurred in two steps include explosive release as well as a slow and stable release. DOX exhibited a continuous and fast release in the first 5 h. After that, the release rate was slowed down and finally the cumulative release of DOX reached nearly 69% at 24 h.

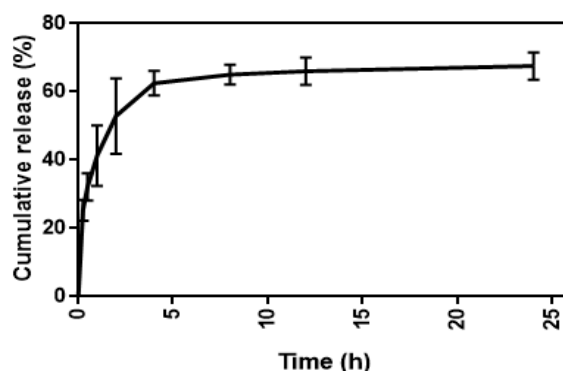


Figure 4. In vitro DOX release profile from DOX-loaded micelle at pH 7.4 for 24 h (mean \pm SD, n=3).

• Biocompatibility of polymeric micelles

To evaluate the biocompatibility of polymeric micelles, MTT cell assay was performed against the MCF7 and HepG2 cell lines at different concentrations (ranging from 12.5 to 800 μ g/ml) of nanoparticles. As shown in Fig 5 no significant cytotoxicity of blank nanocarriers were observed for concentrations below 800 μ g /ml and 400 μ g /ml in MCF7 and HepG2 cell lines, respectively.

• In vitro cytotoxicity

MCF7 and HepG2 cells were treated for 24 h at various DOX concentrations ranging from 0.0 to 5 μ g/ml. Fig 6 shows the cell viability of MCF7 cells and its significant relationship with the control sample (zero concentration of DOX). As shown in the figure, at all DOX concentrations a significant toxicity effect was observed on MCF7 cells compared to control cells ($P < 0.0001$) and was quite significant. The cell viability decreased obviously as the micelle concentration increased. DOX-loaded micelle and free DOX induced cytotoxic effects in 24 hours. At the highest investigated DOX concentration (5 μ g/ml), the viabilities of MCF7 cells treated with DOX-

loaded micelle further dropped to 29%, while that was 41% for free DOX treated cells. As shown in [Fig 7](#) DOX-loaded micelles showed comparable antitumor activity to the free DOX in HepG2 cells at low concentration of DOX, but at highest DOX concentration (5 $\mu\text{g/ml}$), compared to Free DOX, micelles exhibited lower toxicity against HepG2 cells.

The half-maximal inhibitory concentration (IC₅₀) of free DOX and DOX-loaded micelles after 24 h was investigated. It was found that IC₅₀ value of DOX-loaded micelles against MCF7 cells was approximately 0.5 $\mu\text{g/ml}$, that was lower than that of free DOX (more than 0.5 $\mu\text{g/ml}$). In contrast,

the IC₅₀ value of DOX-loaded micelles against HepG2 cells was higher than free DOX.

• Cellular uptake

The MCF7 cells were used to assess the cellular uptake of DOX. As a result, [Fig 8](#) clearly showed that the cellular uptake of DOX-loaded micelles were higher than that of the free-DOX.

• Apoptosis assay

Flow cytometry data show that after treatment with the DOX and DOX-loaded micelles, the ratio of apoptotic cells in MCF7 cells are 19.1% and 32.8%, respectively ([Fig 9](#)).

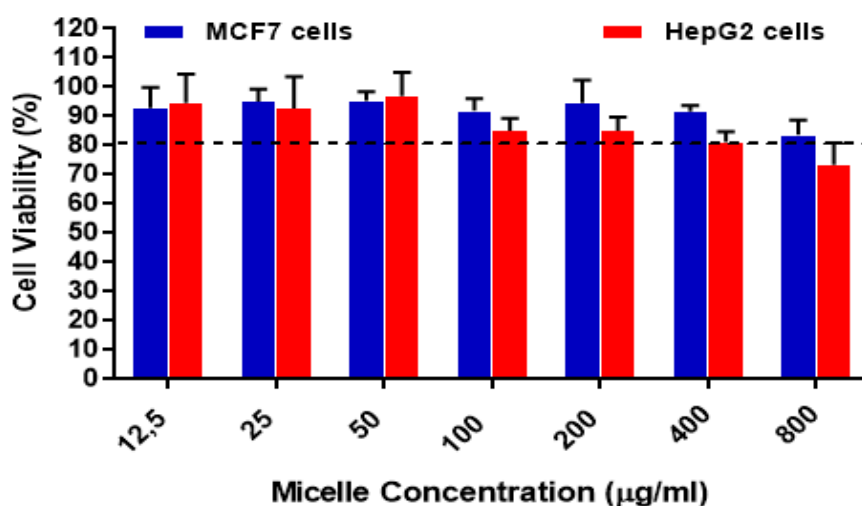


Figure 5. The cytotoxicity of PBMA-b-POEGMA micelle against MCF-7 and HepG2 cells. Data presented as mean \pm SD (n=3)

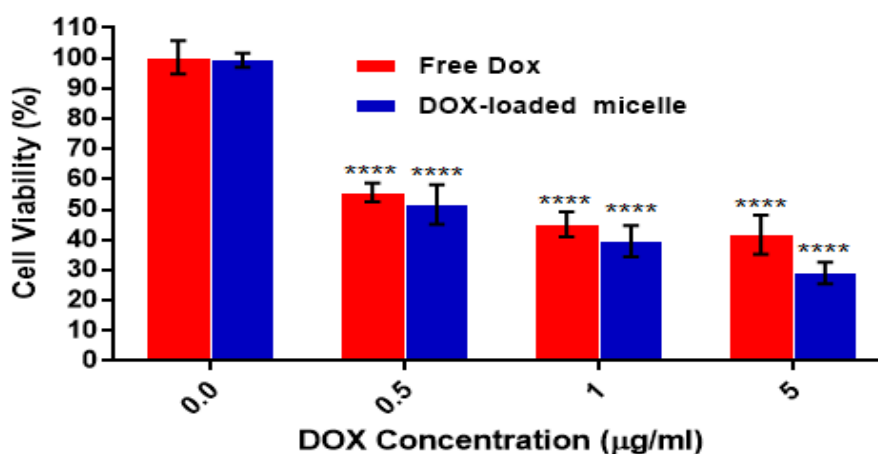


Figure 6. The cell viability of MCF7 cancer cells after treatment with free DOX and DOX-loaded micelles for 24h. Data presented as mean \pm SD (n=3), Bar marked with **** (P<0.0001) showed significant difference compared to the control group (0.0 concentration of DOX).

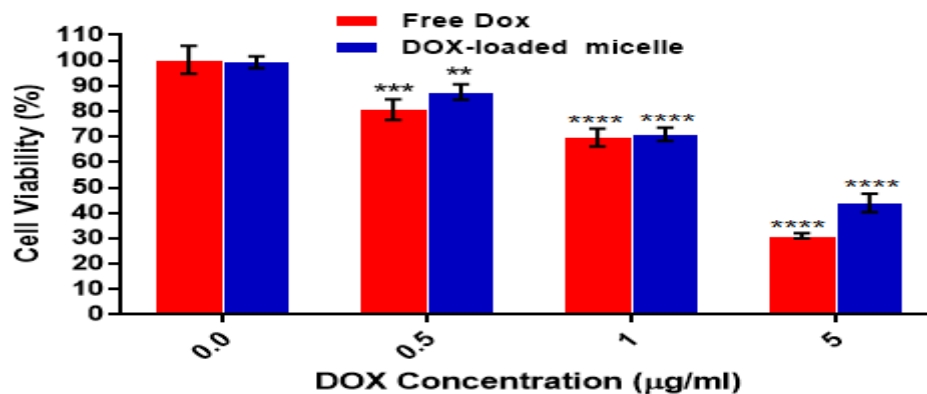


Figure 7. The cell viability of HepG2 cancer cells after treatment with free DOX and DOX-loaded micelles for 24h. Data presented as mean \pm SD (n=3), Bar marked with **** (P<0.0001), *** (P<0.001), and ** (P<0.01) showed significant difference compared to the control group (0.0 concentration of DOX).

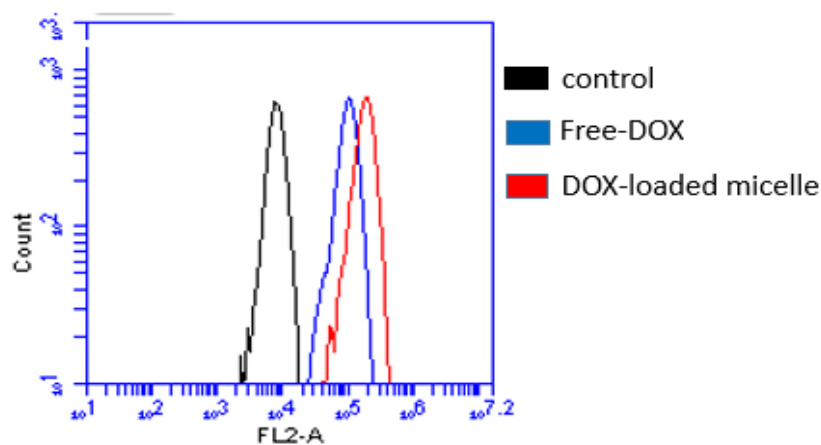


Figure 8. Cell uptake study of free DOX and DOX-loaded micelles after incubation with MCF7 cell lines for 4 h with DOX concentration of 5 µg/mL.

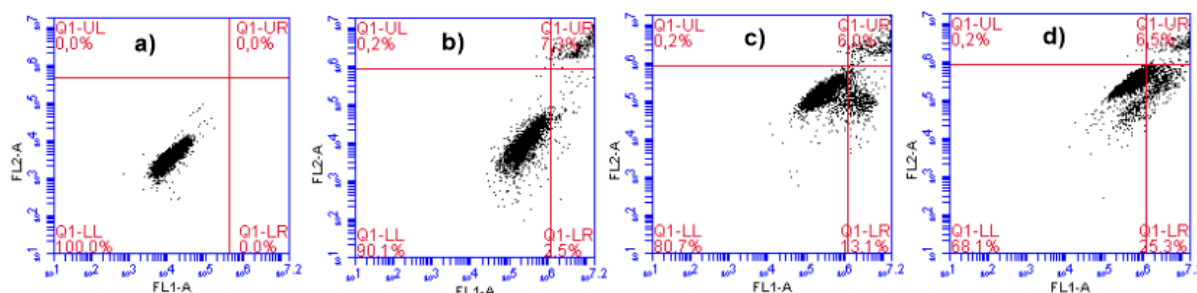


Figure 9. Cell apoptosis of MCF7 cells incubated with a) unstained, b) control, c) Free-DOX, and d) DOX-loaded micelle for 24 h (DOX concentration of 5 µg/mL) analyzed by flow cytometry.

Discussion

PBMA-b-POEGMA diblock copolymers were synthesized via RAFT polymerization. The shorter retention time in GPC chromatograms showed the efficient chain extension from PBMA block and the formation of PBMA-b-POEGMA

block copolymers. The relatively low polydispersity of polymer indicate that RAFT polymerization of PBMA-b-POEGMA leads to the synthesis of well-defined copolymers. As can be seen this amphiphilic diblock copolymer self-assembled into narrow distributed ranged-size

micelles, which is in good agreement with previous works (24, 25). Based on the studies, the size of the nanocarriers is one of the main factors to deliver drug agents to the target sites because the body's immune system quickly removes massive particles. In this regard, the drug-loaded nanocarriers with average diameters less than 200 nm can be easily transferred to target sites through the circulatory system (26, 27). Moreover, the parameter of the polydispersity index (PDI) was assessed to measure the width of particle size distribution and the required PDI for pharmaceutical nanoparticles is less than 0.35 (28), based on the results, it seems that polymeric micelle can be suitable for drug delivery applications. Here the hydrophobic anticancer drug DOX was loaded into the core of the micelles in order to overcome the mentioned limitations and improve the anticancer efficacy of DOX (29, 30). It should be noted that the size, polydispersity of loaded micelles, and the loading efficiency, depend on the drug-polymer weight ratio (31, 32). Studies showed that the increase of this ratio leads to an increase in drug loading content (DLC) and drug loading efficiency (DLE), that related to the increase of weight of drug-loaded micelle compacted to weight micelle, and with the increase of the ratio of drug-copolymer, the particle size increased, which might be explained by the enhancement of intermolecular forces of drug-loaded nanocarrier.

The release profiles of DOX from micelles were conducted at different times in the PBS solution at pH 7.4. This increased release of DOX from the micelle could be attributed to the hydrophobic interaction between the drugs and hydrophobic core. It was found that the release of DOX from the micelles was a mixed effect of diffusion and disintegration. It might be explained to the diffusion of the drug from the hydrophobic core and the disintegration of the polymeric shell (33).

MTT results proved that this polymeric micelle is biocompatible and can be used as a biomaterial for nanomedicinal application. The anticancer activity of the DOX-loaded micelles was investigated against MCF7 and HepG2 cells by MTT assay. Because in the same concentrations

of drug the DOX-loaded micelle showed higher cytotoxic effects against MCF7 cells in comparison with free DOX. In this way, the side effects are assumed to be less than usual free higher dose administrations, due to the decrease the dose of the drug. Similar results were obtained with incubation of DOX against drug-sensitive MCF7 cells in other formulations (34-36). Zhou et al developed DOX-loaded redox-responsive (DEX-SS-IND) micelles, and these micelles exhibited a comparatively lower IC50 value than the drug in MCF7 cells (34). Cuong et al confirmed that the optimal treatment time for cell viability assay of DOX-loaded PEG-PCL-PEG micelle was approximately 48 h, and confocal microscopy indicated that DOX was internalized into the cytoplasm via endocytosis (35). Based on our results, PBMA-b-POEGMA micelles showed relatively high cytotoxicity with 24 h incubation, due to presence of POEGMA that enhanced the internalization into cells. Hong et al evaluated multifunctional micelles in DOX-sensitive MCF7 cells and DOX-resistant MCF7/ADR cells. Active targeting and active targeting in combination with endo-lysosomal escape have been demonstrated to be the primary function for a micelle against doxorubicin-sensitive and doxorubicin-resistant cells, respectively (36). In our study, the increased anticancer activity of DOX-loaded micelles in MCF7 cells can be attributed to the presence of POEGMA shell on the surface which enhanced the uptake mediated through endocytosis, and well-defined polymeric micelle with nano-size that led to passive targeting of drug. These results confirm that PBMA-b-POEGMA micelles are more effective on MCF7 breast cancer cells than HepG2 cells, therefore, the DOX-loaded polymeric micelles have been demonstrated to be potential nanocarriers for effective delivery drug to breast cancer cells.

Since the DOX-loaded micelles exhibited much more potent cytotoxicity against MCF7 cells than free DOX, we choose this cell line for further investigations. Flow cytometry is a reliable method that provides quantitative information about the uptake of fluorescently labeled

nanoparticles by cells and can measure the accumulation of nanoparticles in cells (23). The cellular uptake of the DOX-loaded micelle was assessed by flow cytometry assay (Fig 9). These results indicate that DOX-loaded micelles can efficiently deliver DOX to MCF7 cells. To decide whether the inhibition of cancer cell proliferation through those DOX-loaded micelles became an outcome of DOX induced apoptosis, we performed the FITC-Annexin V/PI double-staining assay in MCF7 cells. As can be seen, the DOX-loaded micelles induce a far higher level of apoptosis in MCF7 cells with an equivalent dose, which is consistent with MTT and cellular uptake results. Induction of programmed death is one of the methods in killing cancer cells and the use of nanoparticles in this context is increasing. In the present study it was shown that polymeric micelles were able to creating induced programmed death in MCF7 cells. Investigate this type of death induced by polymeric micelles showed that this nanoparticle conducts MCF7 cells to apoptosis and the tendency of this nanoparticle to penetrate cancer cells. The effectiveness of these nanoparticles on the cancer cells can be attributed to their small size.

Conclusion

Amphiphilic block copolymers of PBMA-b-POEGMA for enhanced drug delivery applications were successfully synthesized using RAFT polymerization technique. The molecular weights of synthesized homopolymer (PBMA) and block copolymer were found to be 12000 and 28000 gmol⁻¹, respectively. The relatively low polydispersity of polymers indicate the efficiency of RAFT polymerization in the synthesis of well-defined polymers. The self-assembly behavior of the block copolymer was investigated by TEM and DLS. The average sizes of the polymeric blank micelles and DOX-loaded micelles were obtained to be 35 nm and 45nm, respectively. The synthesized block copolymer exhibited excellent DOX-loading capacity (50 ±3.46 %) and the release of DOX from the micellar nanocarriers reached nearly 69% at 24 h. The biocompatibility of the block copolymer was confirmed through

the MTT assay against MCF7 and HepG2 cell lines. The DOX-loaded polymeric micelle showed higher anticancer efficacy compared with free DOX against MCF7 verified by MTT, cellular uptake, and apoptosis assays.

References

1. Torchilin VP. Recent advances with liposomes as pharmaceutical carriers. *Nat Rev Drug Discov.* 2005; 4(2):145. [[view at publisher](#)] [[DOI](#)] [[PMID](#)] [[Google Scholar](#)]
2. Shuai X, Ai H, Nasongkla N, Kim S, Gao J. Micellar carriers based on block copolymers of poly (ϵ -caprolactone) and poly (ethylene glycol) for doxorubicin delivery. *J Control Release.* 2004;98(3):415-26. [[view at publisher](#)] [[DOI](#)] [[PMID](#)] [[Google Scholar](#)]
3. Liu Y, Li L-L, Qi G-B, Chen X-G, Wang H. Dynamic disordering of liposomal cocktails and the spatio-temporal favorable release of cargoes to circumvent drug resistance. *Biomaterials.* 2014;35(10):3406-15. [[view at publisher](#)] [[DOI](#)] [[PMID](#)] [[Google Scholar](#)]
4. Chung M, Chen K, Liang H, Liao Z, Chia W, Xia Y, et al. A liposomal system capable of generating CO₂ bubbles to induce transient cavitation, lysosomal rupturing, and cell necrosis. *Angew Chemie Int Ed.* 2012;51(40):10089-93. [[view at publisher](#)] [[DOI](#)] [[PMID](#)] [[Google Scholar](#)]
5. Han S, Liu Y, Nie X, Xu Q, Jiao F, Li W, et al. Efficient Delivery of Antitumor Drug to the Nuclei of Tumor Cells by Amphiphilic Biodegradable Poly (L-Aspartic Acid-co-Lactic Acid)/DPPE Co-Polymer Nanoparticles. *Small.* 2012;8(10):1596-606. [[view at publisher](#)] [[DOI](#)] [[PMID](#)] [[Google Scholar](#)]
6. Maeda H, Nakamura H, Fang J. The EPR effect for macromolecular drug delivery to solid tumors: Improvement of tumor uptake, lowering of systemic toxicity, and distinct tumor imaging in vivo. *Adv Drug Deliv Rev.* 2013; 65(1):71-9. [[view at publisher](#)] [[DOI](#)] [[PMID](#)] [[Google Scholar](#)]

7. Discher DE, Eisenberg A. Polymer vesicles. *Science* (80-). 2002; 297(5583):967-73. [[DOI](#)] [[PMID](#)]
8. Burke SE, Eisenberg A. Kinetics and mechanisms of the sphere-to-rod and rod-to-sphere transitions in the ternary system PS310-b-PAA52/dioxane/water. *Langmuir*. 2001; 17(21):6705-14. [[view at publisher](#)] [[DOI](#)] [[Google Scholar](#)]
9. Matsumura Y, Maeda H. A new concept for macromolecular therapeutics in cancer chemotherapy: mechanism of tumoritropic accumulation of proteins and the antitumor agent smancs. *Cancer Res*. 1986;46(12 Part 1):6387-92. [[view at publisher](#)] [[Google Scholar](#)]
10. Matsumura Y, Hamaguchi T, Ura T, Muro K, Yamada Y, Shimada Y, et al. Phase I clinical trial and pharmacokinetic evaluation of NK911, a micelle-encapsulated doxorubicin. *Br J Cancer*. 2004;91(10):1775. [[view at publisher](#)] [[DOI](#)] [[PMID](#)] [[PMCID](#)] [[Google Scholar](#)]
11. Hwang D, Ramsey JD, Kabanov A V. Polymeric micelles for the delivery of poorly soluble drugs: from nanoformulation to clinical approval. *Adv Drug Deliv Rev*. 2020; [[view at publisher](#)] [[DOI](#)] [[PMID](#)] [[Google Scholar](#)]
12. Lin J, Peng C, Ravi S, Siddiki AKM, Zheng J, Balkus KJ. Biphenyl wrinkled mesoporous silica nanoparticles for pH-responsive doxorubicin drug delivery. *Materials (Basel)*. 2020;13(8):1998. [[view at publisher](#)] [[DOI](#)] [[PMID](#)] [[PMCID](#)] [[Google Scholar](#)]
13. Gomaa EA, Morsi MA, Negm AE, Sherif YA. Cyclic voltammetry of bulk and nano manganese sulfate with Doxorubicin using glassy Carbon electrode. *Int J Nano Dimens*. 2017; 8(1):89-96. [[view at publisher](#)] [[Google Scholar](#)]
14. Chen Y, Wan Y, Wang Y, Zhang H, Jiao Z. Anticancer efficacy enhancement and attenuation of side effects of doxorubicin with titanium dioxide nanoparticles. *Int J Nanomedicine*. 2011;6: 2321. [[DOI](#)] [[PMID](#)] [[PMCID](#)] [[Google Scholar](#)]
15. Cabeza L, Ortiz R, Arias JL, Prados J, Martínez MAR, Entrena JM, et al. Enhanced antitumor activity of doxorubicin in breast cancer through the use of poly (butylcyanoacrylate) nanoparticles. *Int J Nanomedicine*. 2015;10:1291. [[view at publisher](#)] [[DOI](#)] [[PMID](#)] [[PMCID](#)] [[Google Scholar](#)]
16. He S, Zhou Z, Li L, Yang Q, Yang Y, Guan S, et al. Comparison of active and passive targeting of doxorubicin for somatostatin receptor 2 positive tumor models by octreotide-modified HPMA copolymer-doxorubicin conjugates. *Drug Deliv*. 2016; 23(1):285-96. [[view at publisher](#)] [[DOI](#)] [[PMID](#)] [[Google Scholar](#)]
17. York AW, Kirkland SE, McCormick CL. Advances in the synthesis of amphiphilic block copolymers via RAFT polymerization: stimuli-responsive drug and gene delivery. *Adv Drug Deliv Rev*. 2008; 60(9):1018-36. [[view at publisher](#)] [[DOI](#)] [[PMID](#)] [[Google Scholar](#)]
18. Jia Z, Wong L, Davis TP, Bulmus V. One-Pot Conversion of RAFT-Generated Multifunctional Block Copolymers of HPMA to Doxorubicin Conjugated Acid- and Reductant-Sensitive Crosslinked Micelles. 2008; 3106-13. [[view at publisher](#)] [[DOI](#)] [[PMID](#)] [[Google Scholar](#)]
19. Boyer C, Bulmus V, Davis TP, Ladmiral V, Liu J, Perrier S. Bioapplications of RAFT polymerization. *Chem Rev*. 2009; 109(11):5402-36. [[view at publisher](#)] [[DOI](#)] [[PMID](#)] [[Google Scholar](#)]
20. Khan M, Guimarães TR, Choong K, Moad G, Perrier S, Zetterlund PB. RAFT Emulsion Polymerization for (Multi) block Copolymer Synthesis: Overcoming the Constraints of Monomer Order. *Macromolecules*. 2021; 54(2):736-46. [[view at publisher](#)] [[DOI](#)] [[Google Scholar](#)]
21. Du Y, Jia S, Chen Y, Zhang L, Tan J. Type I Photoinitiator-Functionalized Block Copolymer Nanoparticles Prepared by RAFT-Mediated Polymerization-Induced Self-Assembly. *ACS Macro Lett*. 2021; 10(2):297-306. [[view at publisher](#)] [[DOI](#)] [[Google Scholar](#)]

22. Lo CL, Huang CK, Lin KM, Hsiue GH. Mixed micelles formed from graft and diblock copolymers for application in intracellular drug delivery. *Biomaterials*. 2007; 28(6):1225-35. [[view at publisher](#)] [[DOI](#)] [[PMID](#)] [[Google Scholar](#)]
23. Ghorbani M, Mahmoodzadeh F, Nezhad-Mokhtari P, Hamishehkar H. A novel polymeric micelle-decorated Fe₃O₄/Au core-shell nanoparticle for pH and reduction-responsive intracellular co-delivery of doxorubicin and 6-mercaptopurine. *New J Chem*. 2018; 42(22):18038-49. [[view at publisher](#)] [[DOI](#)] [[Google Scholar](#)]
24. Guo X, Zhao Z, Chen D, Qiao M, Wan F, Cun D, et al. Co-delivery of resveratrol and docetaxel via polymeric micelles to improve the treatment of drug-resistant tumors. *Asian J Pharm Sci*. 2019; 14(1):78-85. [[view at publisher](#)] [[DOI](#)] [[PMID](#)] [[PMCID](#)] [[Google Scholar](#)]
25. Li W, Nakayama M, Akimoto J, Okano T. Effect of block compositions of amphiphilic block copolymers on the physicochemical properties of polymeric micelles. *Polymer (Guildf)*. 2011; 52(17):3783-90. [[view at publisher](#)] [[DOI](#)] [[Google Scholar](#)]
26. Su X, Wang Z, Li L, Zheng M, Zheng C, Gong P, et al. Lipid-polymer nanoparticles encapsulating doxorubicin and 2'-deoxy-5-azacytidine enhance the sensitivity of cancer cells to chemical therapeutics. *Mol Pharm*. 2013; 10(5):1901-9. [[view at publisher](#)] [[DOI](#)] [[PMID](#)] [[Google Scholar](#)]
27. Lv L, Liu C, Chen C, Yu X, Chen G, Shi Y, et al. Quercetin and doxorubicin co-encapsulated biotin receptor-targeting nanoparticles for minimizing drug resistance in breast cancer. *Oncotarget*. 2016;7(22):32184. [[DOI](#)] [[PMID](#)] [[PMCID](#)] [[Google Scholar](#)]
28. Masarudin MJ, Cutts SM, Evison BJ, Phillips DR, Pigram PJ. Factors determining the stability, size distribution, and cellular accumulation of small, monodisperse chitosan nanoparticles as candidate vectors for anticancer drug delivery: application to the passive encapsulation of [14C]-doxorubicin. *Nanotechnol Sci Appl*. 2015; 8:67. [[DOI](#)] [[PMID](#)] [[PMCID](#)] [[Google Scholar](#)]
29. Hazhir N, Chekin F, Raof JB, Fathi S. A porous reduced graphene oxide/chitosan-based nanocarrier as a delivery system of doxorubicin. *RSC Adv*. 2019; 9(53):30729-35. [[view at publisher](#)] [[DOI](#)] [[Google Scholar](#)]
30. Chekin F, Myshin V, Ye R, Melinte S, Singh SK, Kurungot S, et al. Graphene-modified electrodes for sensing doxorubicin hydrochloride in human plasma. *Anal Bioanal Chem*. 2019; 411(8):1509-16. [[view at publisher](#)] [[DOI](#)] [[PMID](#)] [[Google Scholar](#)]
31. Hussein YHA, Youssry M. Polymeric micelles of biodegradable diblock copolymers: enhanced encapsulation of hydrophobic drugs. *Materials (Basel)*. 2018; 11(5):688. [[view at publisher](#)] [[DOI](#)] [[PMID](#)] [[PMCID](#)] [[Google Scholar](#)]
32. Hakemi P, Ghadi A, Mahjoub S, Zabihi E, Tashakkorian H. Ratio Design of Docetaxel/Quercetin Co-Loading-to-Nanocarrier: Synthesis of PCL-PEG-PCL Copolymer, Study of Drug Release Kinetic and Growth Inhibition of Human Breast Cancer (MCF-7) Cell Line. *Russ J Appl Chem*. 2021; 94(3):388-401. [[view at publisher](#)] [[DOI](#)] [[Google Scholar](#)]
33. Phan QT, Le MH, Le TTH, Tran THH, Xuan PN, Ha PT. Characteristics and cytotoxicity of folate-modified curcumin-loaded PLA-PEG micellar nano systems with various PLA: PEG ratios. *Int J Pharm*. 2016; 507(1-2):32-40. [[view at publisher](#)] [[DOI](#)] [[PMID](#)] [[Google Scholar](#)]
34. Zhou Y, Wang S, Ying X, Wang Y, Geng P, Deng A, et al. Doxorubicin-loaded redox-responsive micelles based on dextran and indomethacin for resistant breast cancer. *Int J Nanomedicine*. 2017;12: 6153. [[DOI](#)] [[PMID](#)] [[PMCID](#)] [[Google Scholar](#)]
35. Cuong N-V, Jiang J-L, Li Y-L, Chen J-R, Jwo S-C, Hsieh M-F. Doxorubicin-loaded PEG-PCL-PEG micelle using xenograft model of nude mice: Effect of multiple administration of micelle on the suppression of human breast cancer. *Cancers*

(Basel). 2011; 3(1):61-78. [[view at publisher](#)]
[[DOI](#)] [[PMID](#)] [[PMCID](#)] [[Google Scholar](#)]

36. Hong W, Shi H, Qiao M, Gao X, Yang J, Tian C, et al. Rational design of multifunctional

micelles against doxorubicin-sensitive and doxorubicin-resistant MCF-7 human breast cancer cells. *Int J Nanomedicine*. 2017; 12:989. [[view at publisher](#)] [[DOI](#)] [[PMID](#)] [[PMCID](#)] [[Google Scholar](#)]

How to cite:

Gharnas-Ghamesh H, Masoumi M, Erfani-Moghadam V. Anticancer Activity of Doxorubicin Loaded PBMA-b-POEGMA Micelles against MCF7 Breast Cancer Cells and HepG2 Liver Cancer Cells; *Jorjani Biomedicine Journal*. 2021; 9(3):49-60.